An Assessment of the Effect of Sea Surfactant on Global Air-Sea CO_2 Fluxes

Wu-ting, Tsai

Department of Civil Engineering, National Chiao Tung University

Kon-Kee Liu

Institute of Oceanography, National Taiwan University

Abstract

It is well known that the presence of surfactants on the water surface, which are ubiquitous in the global ocean, can reduce drastically the gas exchange rate across the air-water interface. Using the recent published monthly global ΔpCO_2 data by Takahashi et al (1997) and the satellite wind speed we assess the effect of surfactants on the global air-sea CO_2 fluxes. Since there exists no global map of surfactant coverage, and it is known that phytoplankton can produce surfactants, we use primary productivity as an indicator of the presence of surfactants. Global ocean primary productivity distribution maps estimated from SeaWIFS ocean color images are used. It is found that within almost half a year (between January and May), the presence of surfactants causes relatively small effect on CO_2 outgasing from global oceans. In contrast, the CO_2 uptake by the oceans is notably suppressed by the presence of surfactants throughout the year. The average reduction in the uptake flux by surfactants is about twice that of outgasing. This results in significant decrease of the net global CO_2 uptake by the ocean.

1. Introduction

The quantitative estimation of the net CO_2 flux across the air-sea boundary of global oceans has recently been the subject of heightened interest and vigorous research. The most direct way to calculate the net CO_2 flux from the ocean to the atmosphere is to integrate the local transfer rate, $F = k \times s \times \Delta pCO_2$, over the global ice-free ocean surface, where k is the transfer velocity of CO_2 across the water-air interface, s is the solubility of CO_2 in bulk water, and $\Delta pCO_2 = pCO_2w - pCO_2a$ is the difference of CO_2 partial pressure across the interface. Uncertainties existing in the calculations include, however, errors in interpolating ΔpCO_2 maps from the limited number of measurements and the variables involved in parameterizing the functional representation of the flux. Efforts to fill the discontinuities in the data and to construct ΔpCO_2 maps have been made using different techniques, such as the numerical interpolation scheme based on the advection fields of Takahashi et al. (1995) and objective mapping of Lefevre (1999). Adjustments, which have been considered to improve the formulation to account for realistic processes, include the thermal skin effect (e.g. Robert and Watson, 1992; Van Scoy et al., 1995) and the chemical enhancement (e.g. Boutin, 1999).

The accumulation of surfactants (surface-active matters) at the water surface induces surface-tension gradients, which then modifies the physical processes underneath. There is considerable experimental evidence to show that the presence of surfactants drastically reduces the rate of gas transport across the water surface (e.g., Goldman et al., 1988; Frew et al., 1990). It is now recognized that such a surfactant effect in retarding gas exchange is hydrodynamic in nature and is caused by the physicochemical interaction between the surfactants and the underlying turbulent flows. Recent numerical validation (Tsai, 1996; 1998) confirms this explanation and shows that an induced boundary layer, which is attributed to the inhomogeneity of surfactant distribution caused by impinging eddies, blocks the intermediate surface renewal processes of the eddies.

In this work, the reduction of gas exchange by natural surfactants, which ubiquitously cover the global ocean surface, are considered in the calculations of CO_2

flux. The aim is to assess the possible impact of the distribution of sea surface surfactants on estimating the global atmosphere-ocean CO_2 flux. Similar study was also conducted by Asher (1997). The data used in the study of Asher (1997), however, were yearly-average climatological maps with very low resolution. The purpose of Asher's work was to demonstrate the possible effects of the surfactant coverage as well the spatial variability of the coverage on the global air-sea CO_2 flux estimates. In addition to the geographical variability, seasonal variability of the surfactant distributions will further complicate the influence of surfactants on the CO_2 flux calculation in that the strong seasonal variabilities in the wind field and the ΔpCO_2 map. In this study, the calculation of Asher (1997) is refined by employing the recently published ΔpCO_2 maps and the satellite wind, SST and ocean color data. Both seasonal and geographical variabilities of the surfactant impact on the global CO_2 fluxes are emphasized.

2. Integration of global CO_2 flux

The transfer velocity, k, which is governed by both turbulent transport and molecular diffusion, depends on the wind velocity U and the Schmidt number $Sc = \nu/D$, where ν is the kinematic viscosity of water and D is the diffusion coefficient of CO_2 in water. Two widely used empirical functional representations of $k = k(U, Sc)$ are: (1) the three-regime, piecewise linear relation between k and U as proposed by Liss and Merlivat (1986), who synthesized and extrapolated the data of the wind-tunnel experiments by Broecker et al. (1978) and the tracer gas (SF_6) exchange experiment of Wanninkhof et al. (1985), and (2) the quadratic dependence of k on U proposed by Wanninkhof (1992) based on the field data of ^{14}C measurements. The Liss and Merlivat (1986) relationship is employed in the calculations here as it was based on data corresponding to processes which take place on much shorter time and space scales compared with those of ^{14}C data. The choice between these two parameterizations of U and k, however, is not critical in this study as the primary objective here is to assess the relative impact of surfactants on the global flux calculations. Moreover, the two relationships more or less coincide after a scaling factor of 1.6 being applied to the quasi-linear relationship (Merlivat et al., 1993).

Much less measured data of k-U relationship in the presence of surfactants are available than for a clean interface. Broecker et al. (1978) measured k for CO_2 in a wind-wave tunnel covered by a monolayer of oleyl alcohol. The measured data of the reduction rate of k due to the presence of surfactants, as reported by Broecker et al. (1978) are taken advantage of here and are extrapolated to the limit of vanishing velocity by fitting the data with a power curve of U. The data fitting finds that the best curve of the reduction rate r is $r = 0.56\,U^{-0.13}$. This reduction rate of k is assumed to be applicable for the regimes of smooth ($U < 3.6$ m/s) and rough (3.6 m/s < U < 10 m/s) water surfaces, identified by Liss and Merlivat (1986). For wind speed above 10 m/s, waves begin to break and the retarding effect of surfactants decreases. The exchange rate is enhanced by bubbles generated in the process of wave breaking, and a similar k-U slope of clean surface is assumed for the surface covered with surfactants, which yields $k = 2.778 \times 10^{-6}(1.04U - 0.12)(Sc/600)^{-2/3}$.

Both the Schmidt number Sc in the k-U relationship and the solubility s depend primarily on water temperature. The solubility of CO_2 in sea water is estimated using the formula derived by Weiss (1974). For the temperature dependence of Schmidt number, it is found that a fourth-order polynomial, rather than the third-order equation given in Wanninkhof (1992), gives better fitting of the data measured by Jahne et al. (1987b) in the temperature ranging from 0 to 40℃. The variation in temperature results in contradictory effects on the Schmidt number and solubility of CO_2. This gives rise to weak temperature dependence on the transfer coefficient $K = k \times s$ (see also Etcheto and Merlivat, 1988).

The surface integration of the local CO_2 flux over the global ice-free ocean surface is discretized by equally dividing the longitude (180°W to 180°E) and the latitude (90°S to 90°N) and approximating the surface by a Hughes rotational ellipsoid.

3. Data

Monthly climatological ΔpCO_2 maps of the global oceans have recently been constructed by Takahashi et al. (1997). The constructions of the maps were based on approximately 250,000 field measurements and an interpolation scheme using a lateral two-dimensional transport model developed by Takahashi et al. (1995). Measurement data which were taken during the El Niño period in the area of the equatorial Pacific between 10°N and 10°S were excluded from the data bin. The resolution of the maps is 4° latitude x 5° longitude.

To obtain monthly climatological wind speed distributions, wind speeds derived from the radiances measured by the Special Sensor Microwave Imager (SSM/I) instrument on board the Defense Meteorological Satellite Program (DMSP) satellites using the algorithm of Wentz (1997) are used in the present study. The data set contains wind vectors, pseudo stress vectors and wind speeds, nominally 10 m above the surface, averaged over five days and 0.5 degrees in latitude and longitude, over the global ice-free oceans between January 1990 and December 1996. The five-day data are averaged into monthly data for a calendar year.

The NOAA/NASA AVHRR Oceans Pathfinder sea surface temperature data (Vazquez, et al., 1996) are

used. The data were derived from the 5-channel Advanced Very High Resolution Radiometer (AVHRR) instrument on board the NOAA -7, -9, -11 and -14 polar orbiting satellites using the NOAA/NASA Pathfinder SST algorithm. The SST data are those that passed the strictest set of test criteria. Again, data cover the period from January 1990 through December 1996. Both wind and SST data were obtained from the NASA Physical Oceanography Distributed Active Archive Center at the Jet Propulsion Laboratory, California Institute of Technology.

The distribution and movement of surfactants is subjected to greater environmental variations than the subsurface water column. Since there exists no global map of surfactant of surfactant coverage, and it is well known that phytoplankton can produce surfactants (e.g. Frew et al., 1990), we use primary productivity as an indicator for the presence of surfactants as in Asher (1997). Global ocean primary productivity distribution maps estimated from SeaWIFS ocean color images using the the semi-analytical model of Behrenfeld and Falkowski (1997) are used. The data were provided by the Ocean Primary Productivity Research Team at the Institute of Marine and Coastal Sciences, Rutgers University.

In that the presence of surfactants is estimated by assuming a threshold value of primary productivity, *pp*, the degree of reduction in the global CO_2 flux is dictated by that chosen threshold value. Three different scenarios of the oceans are considered in the following results and discussions: (1) surfaces which are clean everywhere; (2) surfaces which are considered to be covered with surfactants when $pp > 25$ g-C $m^{-2} mon^{-1}$; and (3) surfaces which are considered to be covered with surfactants when $pp > 15$ g-C $m^{-2} mon^{-1}$.

Geographical variations in the surfactant coverage of the global oceans for January, April, July and October are shown in Figure 1. In general, the surfaces are practically free of surfactants in the central gyres of oceans. In the northern hemisphere, the major regions of surfactant distribution are the subarctic Pacific and Atlantic in boreal summer and autumn (between March and September). In the eastern equatorial and subtropical Pacific and Atlantic waters off the coasts of America and Africa with strong coastal upwelling, the surfaces are covered with surfactants in austral spring and summer (between July and December). In the Indian Ocean, the Arabian Sea and waters off the east coasts of Africa are also covered with surfactants from July to October. The distribution of surfactants in the Southern Ocean begins in July mostly off the west coasts of South Africa, South America and Australia. The area expands and extends eastward, reaching its maximal surfactant coverage in December and January.

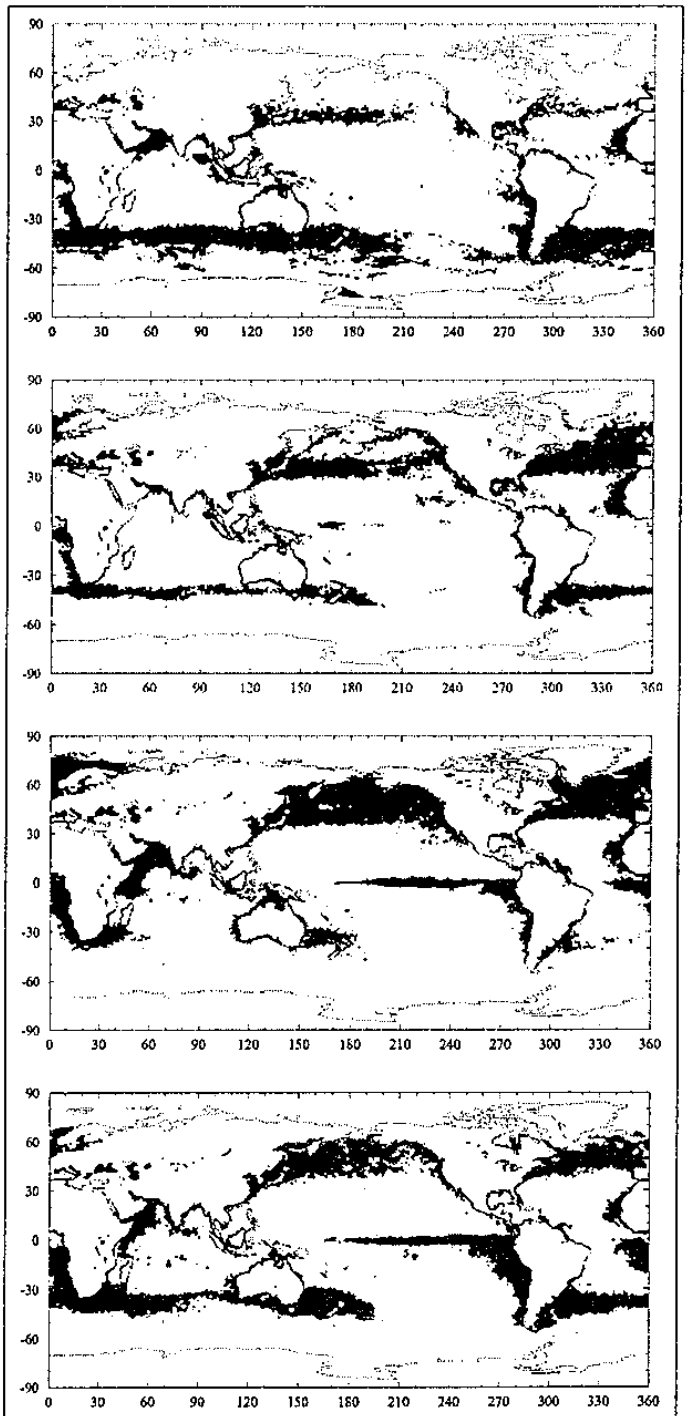

Figure 1. Maps of surfactant coverage of the global oceans for (from top) January, April, July and October with the threshold value of primary productivity $pp = 15$ g-C $m^{-2} mon^{-1}$.

4. Results and Discussion

Figure 2 shows monthly variations in the global average exchange coefficient for the three surface conditions of the oceans. For the clean sea surface, the global exchange coefficient reaches its maximum in July and December. The calculated annual mean of exchange coefficient is 3.24×10^{-2} mol m^{-2} yr^{-1} μatm^{-1}. It becomes 3.30×10^{-2} mol m^{-2} yr^{-1} μatm^{-1} when the

dependence of solubility and the Schmidt number on sea surface temperature are ignored, and the temperature is assumed to be 20℃ as in the calculations of Etcheto et al. (1991). This is close to 3.34×10^{-2} mol m^{-2} yr^{-1} μatm^{-1} as calculated by Etcheto et al. (1991) who also used SSM/I wind speed data (2.5°×2.5° grid resolution). This also validates our calculations.

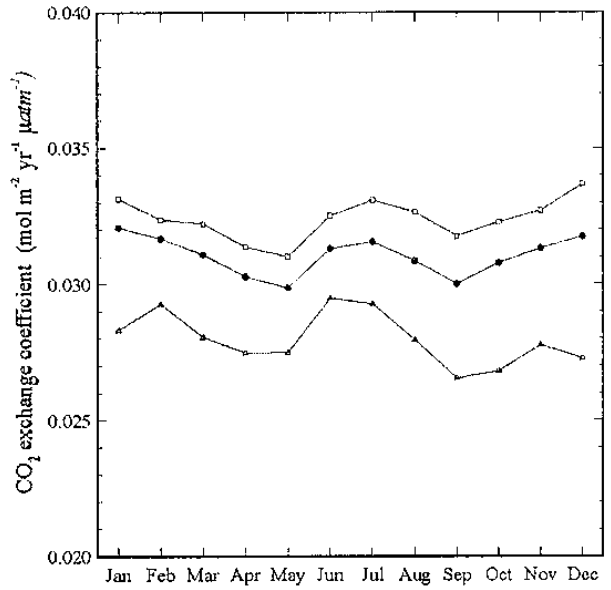

Figure 2. Seasonal variations of the global averaged CO_2 exchange coefficient for the three surface conditions: clean oceans (□); oceans which are classified as surfactant-covered when $pp > 25$ g-C m^{-2} mon^{-1} (●); and when $pp > 15$ g-C m^{-2} mon^{-1} (△).

The degree of reduction caused by the presence of surfactants is approximately constant throughout the seasons for the threshold value of $pp = 25$ g-C m^{-2} mon^{-1}. The global average exchange coefficient decreases from 3.24×10^{-2} mol m^{-2} yr^{-1} μatm^{-1} of the clean ocean to 3.10×10^{-2} mol m^{-2} yr^{-1} μatm^{-1}. In the case of the threshold value of $pp = 15$ g-C m^{-2} mon^{-1}, further reduction occurs and the global average exchange coefficient decreases to 2.80×10^{-2} mol m^{-2} yr^{-1} μatm^{-1}, since the surfactant coverage of ocean surface increases. The most drastic reduction occurs in boreal winter, especially in the months of December and January.

Monthly variations of the global CO_2 net, outgasing and absorption fluxes for the three surface conditions considered are shown in Figure 3. To reveal the geographical variability of the surfactant effect, seasonal variations in the CO_2 fluxes of the major ocean sectors for the three surface conditions are plotted in Figure 4. The global ocean surface is divided into six major sectors: northern (10°N to 70°N) and southern (40°S to 10°N) Pacific sectors, northern (10°N to 70°N) and southern (40°S to 10°N) Atlantic sectors, Indian, Antarctic (south of 40°S), and Arctic sectors (north of 70°N).

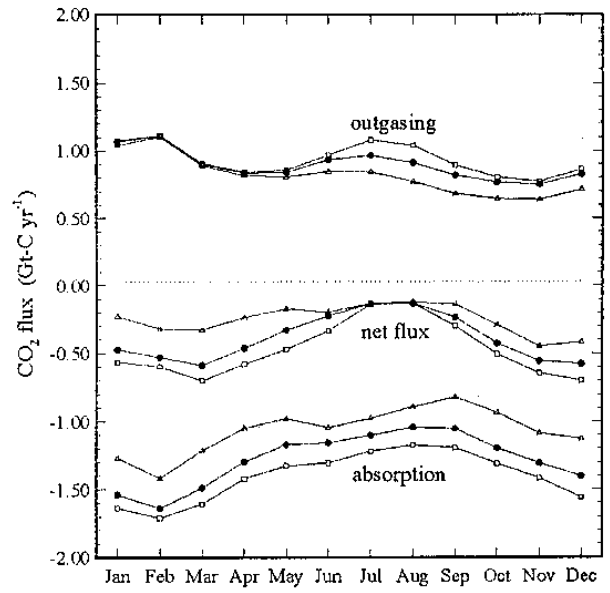

Figure 3. Seasonal variations of the global CO_2 net, outgasing and absorption fluxes for the three surface conditions: clean oceans (□); oceans which are classified as surfactant-covered when $pp > 25$ g-C m^{-2} mon^{-1} (●); and when $pp > 15$ g-C m^{-2} mon^{-1} (△).

For all cases, the net global CO_2 transfer is downward throughout the year. In the case of the clean surface oceans, the net global CO_2 transfer ranges from -0.70 Gt-C/yr in December to -0.13 Gt-C/yr in August. The maxima of both outgasing and absorption fluxes occur in February with values of 1.11 Gt-C/yr and -1.71 Gt-C/yr, respectively. The least outgasing occurs in November with a value of 0.77 Gt-C/yr, whereas the least absorption occurs in August with a value of -1.17 Gt-C/yr. Resolving the global net flux by geographical sectors, as shown in Figure 4, the major uptake occurs in the Antarctic sector throughout the year and in the northern Pacific and Atlantic in boreal winter and spring from November to April. The southern Pacific is the strongest source of CO_2 year round with the maximal release occurring in January.

The distribution of surfactants over the global oceans reduces the monthly CO_2 net flux except in July, during which time the gross surfactant effect virtually vanishes (Fig. 3). The maximal reduction in the net flux occurs in boreal spring (between January and April). Resolving the net flux into outgasing and absorption components, however, reveals interesting features of seasonal variability of the surfactant effect. Within almost half a year (between January and May), the presence of surfactants does not affect CO_2 outgasing from global oceans. By contrast, the CO_2 uptake by the oceans is suppressed by the presence of surfactants throughout the year. In the boreal spring, the lack of corresponding reduction in CO_2 outgasing results in maximal reduction of the net flux. In July, the

reduction in absorption transfer is balanced by a compensatory reduction of outgasing, and the resultant net flux appears unaffected by the presence of surfactants. In fact, the surfactant effect is most noticeable in this time of the year.

The average reduction percentage of absorption transfer by surfactants is about twice that of outgasing for both surfactant coverage conditions. This means that the presence of surfactants suppresses more the uptake of CO_2 by the ocean than its release to the atmosphere. The annual net CO_2 flux is reduced by approximately 20% when the surfactant coverage condition is $pp > 25$ g-C m^{-2} mon^{-1}, and about 50% for the condition $pp > 15$ g-C m^{-2} mon^{-1}.

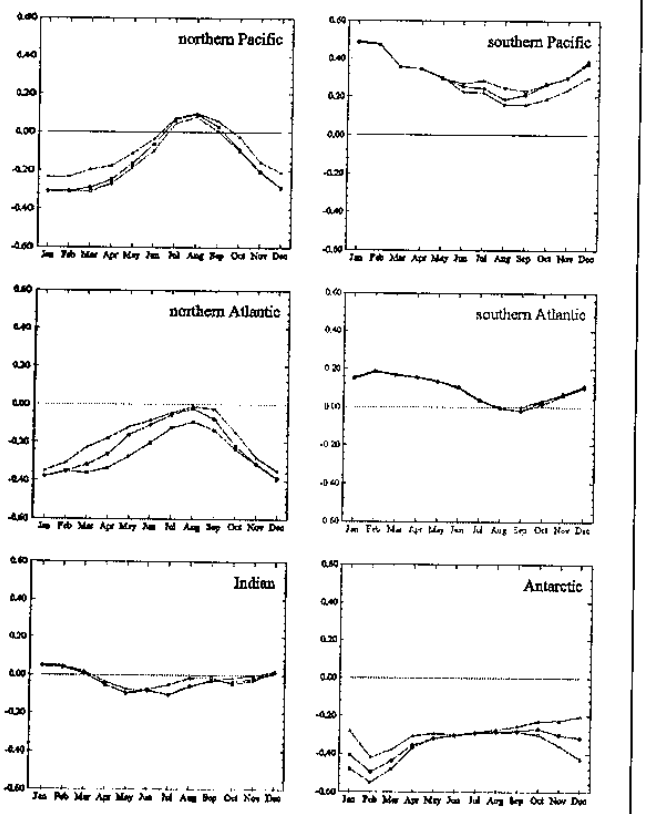

Figure 4. Seasonal variations of the CO_2 net (solid curve), outgasing (long-dashed curve) and absorption (short-dashed curve) fluxes (Gt-C yr^{-1}) in various major ocean sectors for the three surface conditions: clean oceans (□); oceans which are classified as surfactant-covered when $pp > 25$ g-C m^{-2} mon^{-1} (•); and when $pp > 15$ g-C m^{-2} mon^{-1} (△).

In the northern Pacific and Atlantic oceans, the surfactant effect is primarily on suppressing absorption transfer. Such reduction is in effect throughout the year in the northern Pacific and Atlantic (Fig. 4). The major area of surfactant distribution in the northern hemisphere is north of 30°N in the Pacific and Atlantic where the wind-enhanced exchange coefficients are high. In particular, the major reduction of CO_2 uptake occurs along the latitudinal band between 30°N and 50°N of the northwestern Pacific and Atlantic from March to May.

The southern Pacific is a major CO_2 source throughout the year (Fig. 4). The presence of surfactants effectively suppresses the outgasing flux in austral spring and summer (between July and December) and, hence, significantly reduces the positive net flux. In contrast to the northern Pacific and Atlantic, where the magnitudes of flux reduction by surfactants remain finite values throughout the year, the southern Pacific is unaffected by the surfactants for almost half a year (from January to May). Examining the maps of surfactant coverage of the global oceans (Figure 1), it can be seen that there are few biological activities in the southern hemisphere, including the southern Pacific and Atlantic sectors and Indian ocean in the period between January and May.

The most pronounced surfactant effect in the southern Pacific occurs in the eastern equatorial and subtropical waters in the period of austral spring and summer caused by highly productive surface waters off the South American coast. High positive ΔpCO_2 results in strong CO_2 release and, consequently, large outgasing reduction in this region although the degree of reduction in the wind-enhanced transfer rate is not high here. Such pronounced surfactant effects, however, are absent in austral autumn and winter and the eastern equatorial and subtropical Pacific waters remain as a strong CO_2 outgasing source.

In the southern Atlantic sector, the surfactant effect is not as significant as that in the southern Pacific. The decrease in outgasing flux is compensated by the reduction in absorption flux, and the change in net CO_2 flux by the presence of surfactants in the southern Atlantic is rather small.

The Antarctic sector is another major CO_2 sink among the global oceans. Intense biological activities in austral spring and summer, which virtually vanish in fall and winter, result in strong seasonal variability in the absorption flux. As shown in Figure 1, the extent of coverage of surfactants is almost over the entire Antarctic sector in January (and also in November and December). This ensues a significant magnitude of reduction in CO_2 uptake by the Antarctic sector in austral spring and summer.

The Indian ocean is the only sector among the global oceans in which the degrees of CO_2 outgasing and absorption are comparative. As indicated in Figure 1, the major surfactant effects occur in the Arabian Sea and the surface waters off the east coasts of Africa and result in the strong suppression of outgasing flux from July to September (Figure 4). Similar to the southern Pacific sector, the reduction of CO_2 outgasing exceeds absorption from July to September in the Indian Ocean. The total decrease in CO_2 release from the southern Pacific and Indian sectors by the presence of surfactants, however, is not enough to compensate for the reduction in CO_2 absorption by the other ocean sectors.

References

Asher, W. E., The sea-surface microlayer and its effects on global air-sea gas transfer, in *The Sea Surface and Global Change*, edited by P.S. Liss and R.A. Duce, *pp.* 251--286, Cambridge University Press, 1997.

Behrenfeld, M.J. and Falkowski, P.G., Photosynthetic rates derived from satellite-based chlorophyll concentration, *Limnol. Oceanogr.*, *42*, 1-20, 1997.

Boutin, J., Etcheto, J. and Ciais, Possible consequences of the chemical enhancement effects for air-sea CO_2 flux estimates, *Phys. Chem. Earth B*, *24*, 411-416, 1999.

Broecker, H.-C., Petermann, J. and Siems, W., The influence of wind on CO_2-exchange in a wind-wave tunnel, including the effects of monolayers, *J. Marine Res.*, 36, 595-610, 1978.

Etcheto, J., Boutin, J. and Merlivat, L., Seasonal variation of the CO_2 exchange coefficient over the global ocean using satellite wind speeds measurements, *Tellus*, 43B, 247-255, 1991.

Frew, N. M., The role of organic films in air-sea gas exchange, in *The Sea Surface and Global Change*, edited by P.S. Liss and R.A. Duce, *pp.* 121-172, Cambridge University Press, 1997.

Frew, N.M., Goldman, J.C., Dennett, M.R. and Johnson, A.S., Impact of phytoplankton-generated surfactants on air-sea gas exchange, *J. Geophys. Res.*, *95*, 3337-3352, 1990.

Goldman, J.C., Dennett, M.R. and Frew, N.M., Surfactant effects on air-sea gas exchange under turbulent conditions, *Deep-Sea Res.*, *35*, 1953-1970, 1988.

Jahne, B., Munnich, K.O., Bosinger, R., Dutzi, A., Huber, W. and Libner, P., On the parameters influencing air-water gas exchange. *J. Geophys. Res.*, *92*, 1937-1949, 1987a.

Jahne, B., Heinz, G. and Dietrich, W., Measurement of the diffusion coefficients of sparingly soluble gases in water, *J. Geophys. Res.*, *92*, 10767-10776, 1987b.

Lefevre, N., Watson, A.J., Cooper, D.J., Weiss, R.F., Takahashi, T. and Sutherland, S.C., Assessing the seasonality of the oceanic sink for CO_2 in the northern hemisphere, *Global Biogeochem. Cycles*, *13*, 273-286, 1999.

Liss, P.S. and Merlivat, L., Air-sea gas exchange rates: introduction and synthesis. In *The Role of Air-Sea Exchange in Geochemical Cycling*, edited by P. Buat-Menard, *pp.* 113-127, Reidel, 1986.

Merlivat, L. Memery, L. and Boutin, J., Gas exchange at the air-sea interface: present status. Case of CO_2, In *Abstract Volume, 4th International Conference on CO_2*, Carquerainne, France, 1993.

Robertson, J.E. and Watson, A.J., Thermal skin effect of the surface ocean and its implications for CO_2 uptake, *Nature*, *358*, 738-740, 1992.

Takahashi, T., Feely, R.A., Weiss, R.F., Wanninkhof, R.H., Chipman, D.W., Sutherland, S.C. and Takahashi, T.T., Global air-sea flux of CO_2: An estimate based on measurement of sea-air pCO_2 difference, *Proc. Natl. Acad. Sci. USA*, *94*, 8292-8299, 1997.

Takahashi, T., Takahashi, T.T. and Sutherland, S.C. An assessment of the role of the North Atlantic as a CO_2 sink, *Phil. Trans. R. Soc. Lond. B*, 348, 143-152, 1995.

Tsai, W.-T., Impact of a surfactant on a turbulent shear layer under the air-sea interface, *J. Geophys. Res.*, *101*, 28557-28568, 1996.

Tsai, W.-T., Vortex dynamics beneath a surfactant-contaminated ocean surface, *J. Geophys. Res.*, *103*, 27919-27930, 1998.

Van Scoy, K.A., Morris, K.P., Robertson, J.E. and Watson, A.J., Thermal skin effect and the air-sea flux of carbon dioxide: A seasonal high-resolution estimate, *Global Biogeochem. Cycles*, *9*, 253-262, 1995.

Vazquez, J., Tran, A.V., Sumagaysay, R. and Smith, E., *NOAA/NASA AVHRR Oceans Pathfinder Sea Surface Temperature User Reference Manual*, Jet Propulsion Laboratory, Pasadena, CA, 1996.

Wanninkhof, R., Relationship between wind speed and gas exchange over the ocean, *J. Geophys. Res.*, 97, 7373-7382, 1992.

Wanninkhof, R., Ledwell, J.R. and Broecker, W.S., Gas exchange-wind speed relation measured with sulfur hexafluoride on a lake, *Science*, *227*, 1224-1226, 1985.

Weiss, R.F., Carbon dioxide in water and seawater: The solubility of a nonideal gas. *Mar. Chem.*, *8*, 203-215, 1974.

Wentz, F.J., A well-calibrated ocean algorithm for Special Sensor Microwave/Imager. *J. Geophys. Res.*, *102*, 8703-8718, 1997.